IDA

INSTITUTE FOR DEFENSE ANALYSES

Conceptual Design of Low-Signature High-Endurance Hybrid-Electric UAV

Jenya Macheret
Jeremy Teichman
Robert Kraig

November 2011
Approved for public release;
distribution is unlimited.
IDA Document NS D-4496
Log: H 11-001789

The Institute for Defense Analyses is a non-profit corporation that operates three federally funded research and development centers to provide objective analyses of national security issues, particularly those requiring scientific and technical expertise, and conduct related research on other national challenges.

About This Publication

This work was conducted under IDA's independent research program (C2154). The views, opinions, and findings should not be construed as representing the official position of either the Department of Defense.

INSTITUTE FOR DEFENSE ANALYSES

IDA Document NS D-4496

Conceptual Design of Low-Signature High-Endurance Hybrid-Electric UAV

Jenya Macheret
Jeremy Teichman
Robert Kraig

Outline

- Background/Motivation
  - Current UAV endurance limitation
  - Previous work on hybrid electric (HE) UAV
- HE UAV Conceptual Design
  - Current UAVs weight fraction allocation
  - Loiter vs. cruise mission energy tradeoff
  - Visual signature reduction
  - Conceptual design parameters
  - Low acoustic signature operating distance and IR payload
  - Conceptual HE UAV design specifications
- Conclusions
- Backup/Appendix
  - Visual signature analysis
  - IR model description

Selected Examples of Current Small UAVs

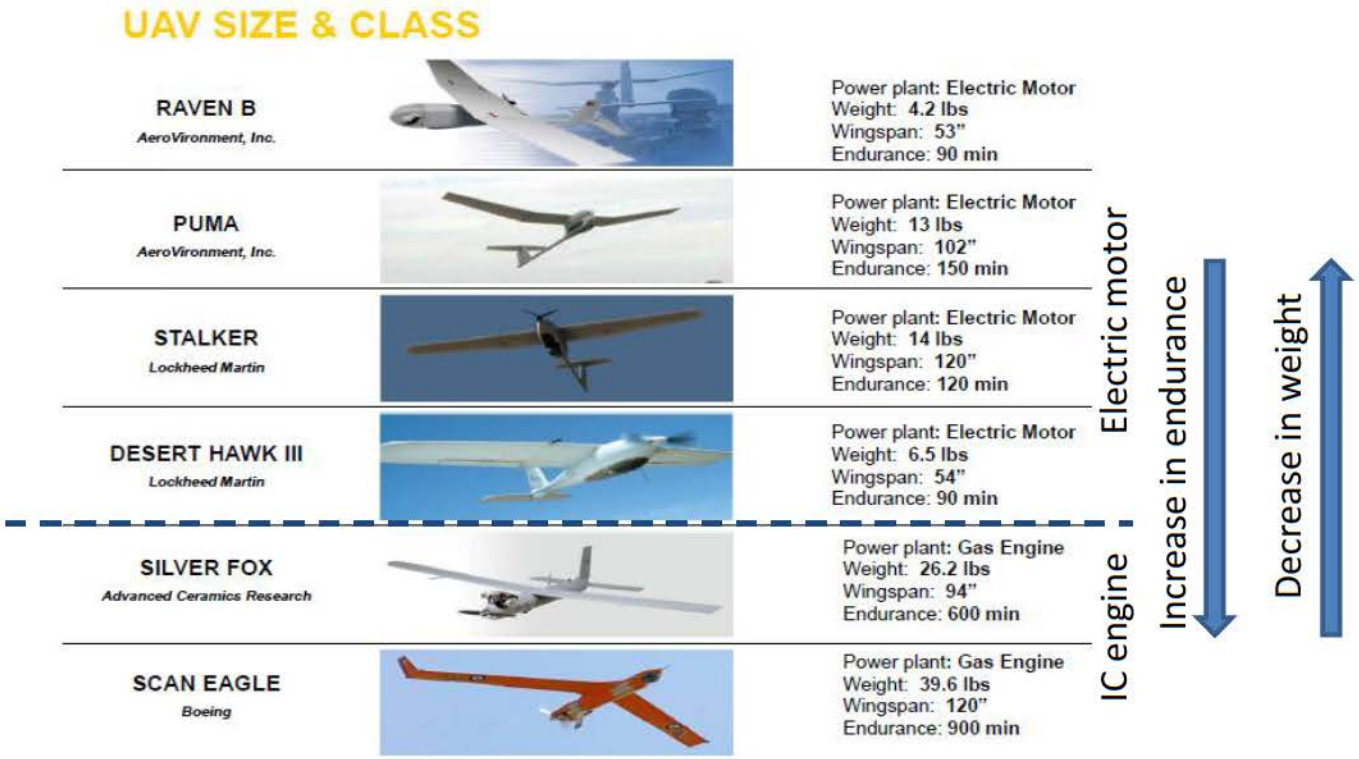

Smaller UAVs are electrically powered; they have low acoustic and visual signatures, but limited endurance; gas-powered UAVs have much longer flight time, but can be easily detected.

The objective of this work: *Investigate feasibility of designing a small hybrid-electric UAV with low acoustic/visual signature and high endurance capabilities*

Small electric UAVs have the advantage of low acoustic and visual signatures, but provide only relatively limited flight endurance. In electric-motor/battery-powered UAV designs, an increase in endurance requires a heavier battery, in turn leading to a heavier UAV. A substantial increase in endurance can also be achieved by employing an internal-combustion engine UAV design, but this configuration results in high noise levels. The objective of this analysis is to answer the question of whether it is feasible to combine the best of the both worlds and build a low acoustic/visual signature UAV with high flight endurance capability.

Selected Examples of Current Small UAV, cont'd

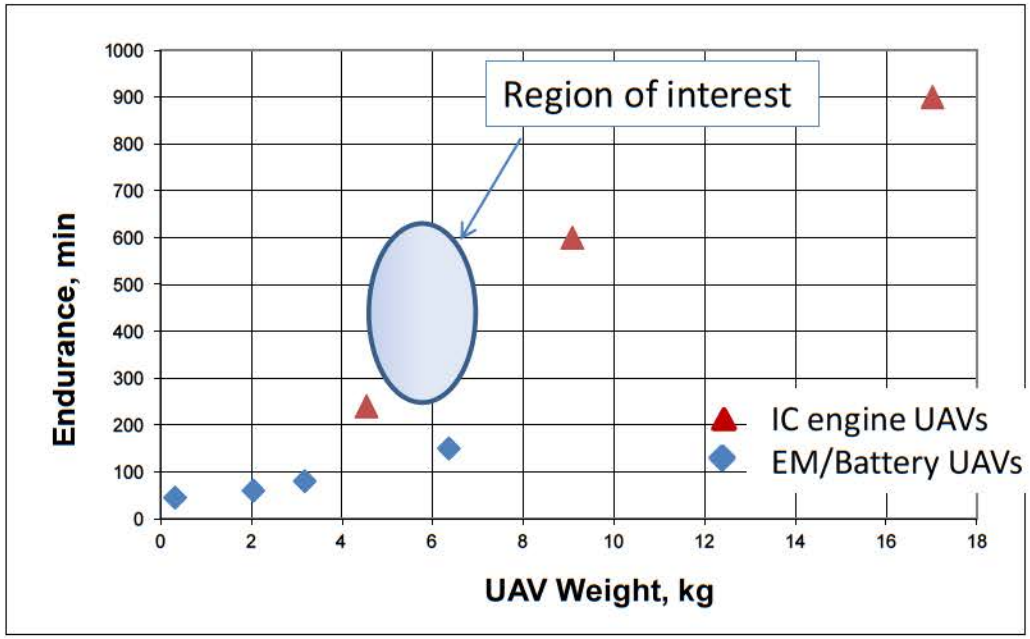

Our report describes a *conceptual design* of a small hybrid electric UAV with low acoustic and visual signatures and high endurance in the design space shown.

The chart plots endurance vs. weight of current electric and gas-powered UAVs. In addition, it identifies the region of interest for the proposed work: 5–7 kg (11–15 lb) with increased endurance. The reason for limiting the UAV weight is that we are interested in hybrid-electric UAVs that will be carried by the soldiers in the field. On the other hand, lighter UAV will have limited endurance. A current UAV in the class weight of our interest is Puma, which, at 13 lb, is reported to have 2–2.5 h endurance. Can this endurance be extended, and if so, by how much?

Why Do We Need a Small, Low Acoustic/Visual Signature, High-Endurance UAV?

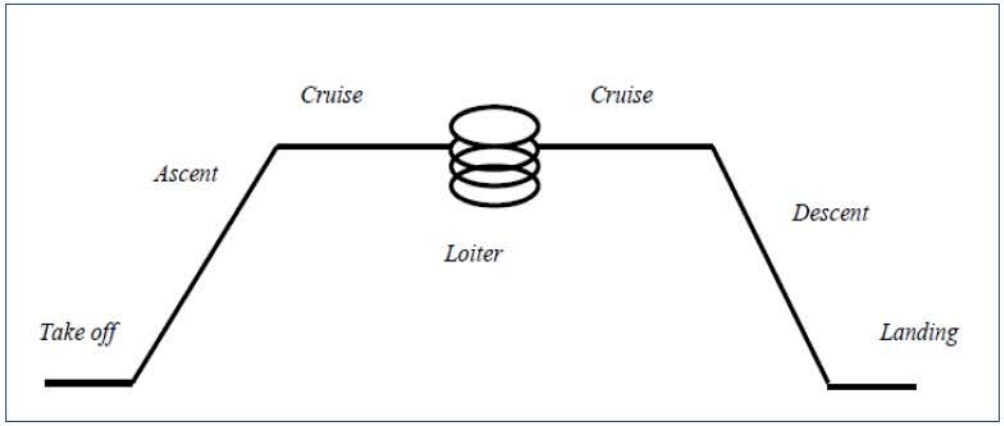

Main idea of this work

IC regime:
- Takeoff
- Ascent/Descent
- Cruise

EM regime:
- Loiter

From IARPA solicitation (http://www.iarpa.gov/solicitation_gho.html)
IARPA seeks to develop technologies and systems *for quiet UAVs that significantly extend the operational time of small ISR UAVs.*
Anticipated innovations include:
hybrid electric propulsion systems that allow for electrically powered flight, ducted propellers systems to reduce … noise sources, flight control systems that manage airframe generated noise, and non-"line of sight" communication systems between the UAV and the ground station.

Our work explores hybrid-electric propulsion systems combined with low-noise and low-visual-signature capabilities; internal-combustion mode is utilized for takeoff, ascent/descent, and cruise portion of the mission; electric-motor propulsion is used for loiter low visual/acoustic signature mission.

Why do we need a small, low acoustic/visual signature, high-endurance UAV? Such UAVs would enable longer range to target and longer loiter missions. The need for such missions is expressed in solicitation by IARPA.

Previous Work on Hybrid-Electric UAV

Parallel Hybrid Electric Configuration with Clutch (the only "conceptually defined "component")#

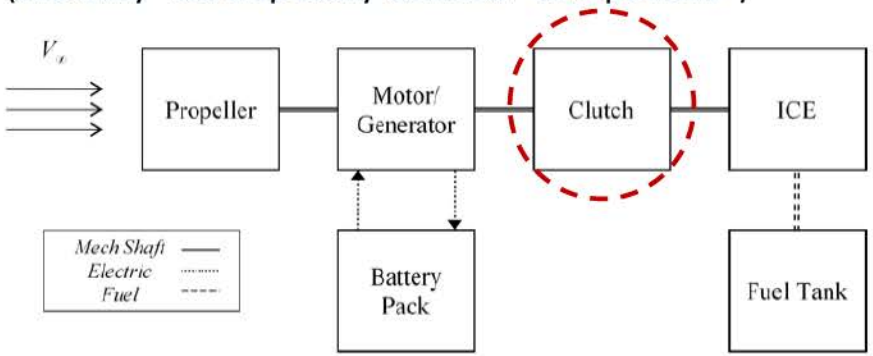

Gearbox/clutch for switching between an IC engine and electric motor*

HE and IC UAV Weight Fractions Comparison##

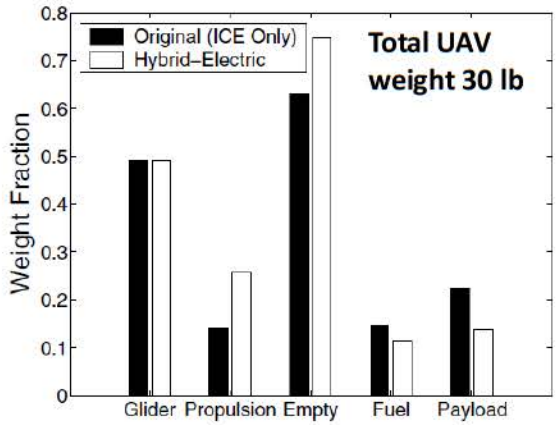

Gearbox developed by the University of Colorado at Boulder and recently licensed to start-up Tigon Enertec:

The "dual torque" hybrid system, called Helios, features a gearbox which allows the internal-combustion engine to provide high power for take off and climb while seamlessly introducing electric power to reduce cruise fuel consumption. The combination reduces the size of engine and weight of batteries needed…*

#R. Hiserote , M.S., Air Force Inst. of Technology, 2010
##F. Harmon at al, JOURNAL OF AIRCRAFT Vol. 43, No. 5, September–October 2006
*Conceptual design document University of Colorado, Team Helios, Sept 24, 1999

Selected hybrid-electric UAVS that have been considered for extending UAV endurance are reported in [1, 2, 3]. In this work, a conceptual design of a 30 lb hybrid-electric UAV with a hybrid drive that consists of an electric motor and internal combustion engine is described. This hybrid-electric UAV is compared with the traditional gas-powered design. As can be seen from the bar chart, some of the fuel and payload of the traditional UAV is replaced by the battery, electric motor, and clutch/gearbox. We did not consider this design for our purposes because of its relatively high weight. In addition, a UAV of this class, powered by an IC engine, has endurance in excess of 10 hours and range that can be extended to thousands of miles. (See for example, Aerosonde UAV, described in [4]). The relative benefits of range/flight endurance extension in this case are not likely to overcome the cost and complexity of the hybrid-electric drive. Another limiting feature of this aircraft was the design of the clutch/gearbox. The authors proposed to have a clutch that connects the internal-combustion engine and electric motor for joint power mode, such as in ascend and high-speed flight. When powered just by the internal-combustion engine without the electric motor, the engine continues to spin the electric motor shaft, adding moment of inertia and mechanical inefficiencies to the drive. In fact, this component seems to be the only one that requires further development in the proposed conceptual design.

A further literature search revealed an option for the clutch/gearbox of the hybrid-electric drive design [5]. This design was developed by a group of students at the University of Colorado. Unfortunately, no detailed description of the design is made available in the open literature. The design has been licensed to a private company, and only a general description can be found in [5]. The gearbox/clutch is about 80% – 85% efficient, and it weighs 2 lb.

References

1. F. Harmon at al, *Journal of Aircraft* Vol. 43, No. 5, September–October 2006.
2. R. Hiserote, Air Force Inst. of Technology, 2010.
3. Rotramel, Air Force Inst. of Technology, 2011.
4. McGeer, *Oceanography*, Vol. 6, No. 3, 1993.
5. Conceptual design document University of Colorado, Team Helios, September 24, 1999.

Basic Design Parameters of Existing UAVs*

		Pointer	Raven	Puma	Dragon eye	Desert Hawk	Orbiter	Metu Guventurk
Span	*m*	2.7	1.4	2.6	1.1	1.32	2.2	2.2
Length	*m*	1.8	1.1	1.8	0.9	0.86	1	1.35
Weight TO	*Kg*	4.095	1.9	5.5	2.3	3.2	5.5	4.5
Weight PL	*kg*	1	0.5	0.9	0.5	0.5	1.2	0.5
Surface	m^2	0.75	0.3	0.832	0.363	0.28	0.611	0.7
Power	*Watt*	300	250	600	400	300	400	900
Velocity_Stall	*m/s*	8.4	8.68	9.22	8.5	11.43	12.75	9
A.R		10	6.7	9	3.33	6.28	7.6	7.5
Endurance	*min*	90	80	120	45	60	2.5	90
Wp/Wto		0.24	0.26	0.16	0.217	0.15	0.27	0.11
hp/W	*hp/N*	0.01	0.0134	0.014	0.0237	0.0128	0.0099	0.027
W/S	N/m^2	53.56	62.13	64.84	62.16	112	104.25	63.06

Main idea:
Substitute electric motor/battery with a hybrid-electric propulsion system in a Puma-sized UAV

*G. Landolfo, PhD, University of Dayton, May 2008

Our idea is to consider Puma UAV parameters as the baseline for our conceptual design. The question then become whether it is possible to design a high-endurance UAV of Puma size by replacing Puma's electric drive electric motor/battery by a hybrid-electric drive consisting of electric motor/battery, internal-combustion engine/gearbox, and fuel. We anticipate that such a design will not necessarily be an optimum one. Our aim, instead, is to show that a design space for such a UAV exists and at least one conceptual design can be found. More detailed designs can then be performed with the goal of finding an optimum one. The optimum design can be defined relative to desired mission. For example, a design can be optimized with respect to loiter endurance.

Preliminary HE UAV Design: Propulsion System Considerations

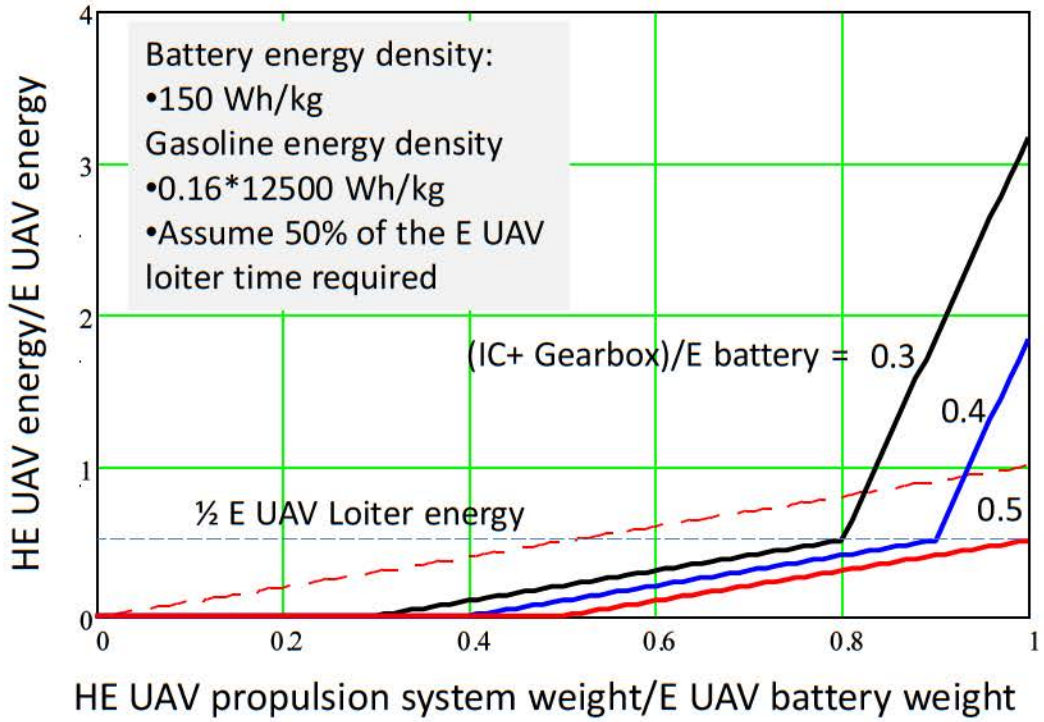

"Back of the envelope" calculations show when the proposed design makes sense: the (internal-combustion engine + Gearbox) weight should be about (or less) 0.4 weight of the original E UAV battery.

Note the desired loiter/cruise time mission requirements can be achieved by the tradeoff between the weight of the battery and that of gas on board.

To determine what weight combinations of battery, internal-combustion engine, and gearbox would result in a feasible design, we consider ratio of the hybrid-electric UAV to electric UAV (E UAV) total energy on board available as a function of the ratio of the hybrid-electric UAV Propulsion system to E UAV battery weight. (We define propulsion system weight as a sum of the internal-combustion engine plus gearbox weight.) Given current battery and gasoline energy densities, substituting part of the electric UAV battery by the propulsion system and fuel results in the following energy trade-offs. Assuming that at least half the loiter energy of the E UAV is required for hybrid-electric UAV, we replace one-half of the E UAV battery by the hybrid-electric UAV propulsion weight and fuel. In this case, the lighter the propulsion, the more fuel can be put on board, and the more total energy is available on board. As can be seen from the figure, when the propulsion is one-third of the total E UAV battery weight, the total energy on board of the hybrid-electric UAV is over three times that of the E UAV. Keep in mind however, that the loiter (i.e., electric) energy available is still only one-half of that of the E UAV. The excess of the total energy on-board will be then utilized for the cruise (IC powered) portion of the mission. For heavier propulsion systems, the advantages of the hybrid-electric design diminish rapidly. When the propulsion weighs one-half the E UAV battery, the hybrid-electric UAV loses half the E UAV loiter energy without any energy gains.

Basic Design Parameters of Existing UAVs,* (cont'd.)

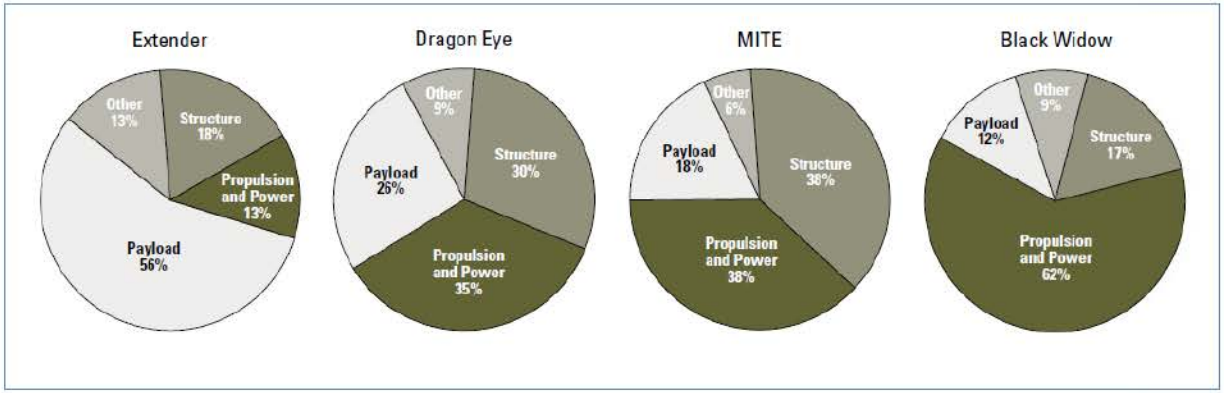

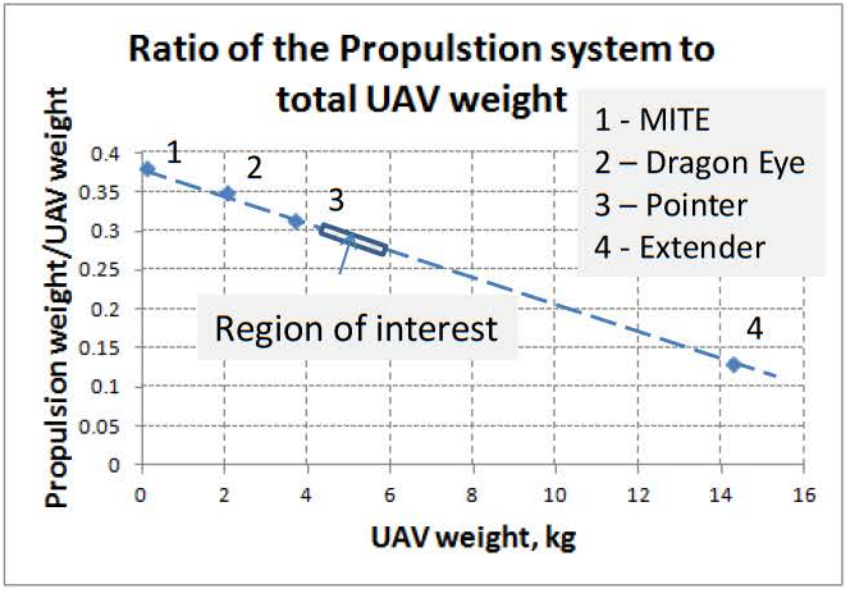

*T. Coffey, Defense Horizons, December 2002

The exact weight of Puma's battery is not available in the open literature. To estimate it, we consider battery-to-total-UAV-weight fractions for various UAV designs, as shown on the figure.

The Puma weighs 5.5 kg, and we estimate the weight of its battery to be about 1.7 kg. For our hybrid-electric UAV design, we consider an option of using a 2 kg battery. With the ratio of battery to total weight at 0.3, we arrive at the total UAV weight of 6.6 kg (14 lb). As an example, consider a hybrid-electric UAV with 1 kg of electric battery, with 1 kg left for propulsion system and fuel. An internal-combustion engine for such an aircraft can be found [1]. OS FS-40S four-stroke, with 480 W power, weighing 350 g is currently available. Considering that a 30 lb aircraft requires about 500 W at cruise speed of 22–25 m/s, such an engine should provide sufficient power for the 14 lb aircraft in this speed range.[1]

[1] R. Hiserote, Air Force Inst. of Technology, 2010

Trade-off Between Loiter and Cruise Energy of Hybrid-Electric UAV: An Example

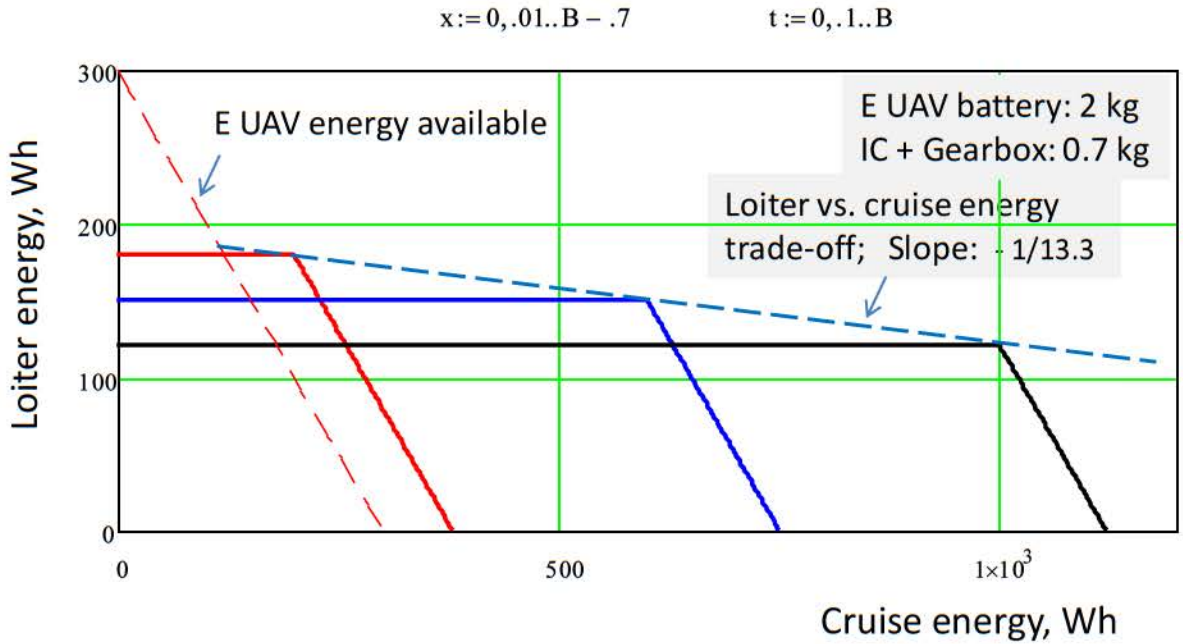

Note that battery choice affects ratio of loiter to cruise mission time; lighter internal-combustion engine and gearbox will lead to more advantageous hybrid-electric UAV trade-offs, but may not provide enough power for the cruise portion of the mission. The problem can be posed as follows:

Maximize loiter time for a given cruise energy and multiple UAV design constraints.

With the total weight of the battery, propulsion system, and fuel at 2 kg, and 700 grams of the propulsion system weight, the trade-off between available loiter and cruise energies can be performed by trading the battery and fuel weights. As shown in the figure, at 1 kg battery, the hybrid-electric UAV offers one-half the loiter energy, but the cruise energy is extended to 750 Wh, compared with 300 Wh of the E UAV.

The slope of the trade-off line is equal to –1/13.3, which is determined by the ratio of the gasoline energy multiplied by internal-combustion engine efficiency (0.16* 12500 = 2000 Wh/kg) to the energy density of the battery (150 Wh/kg). So, for every 1 Wh loss of loiter energy, the hybrid-electric UAV gains about 13.3 Wh of cruise energy. The height of the trade-off line depends on the weight of the propulsion system: the lower the weight, the higher the line and the higher the loiter energy available for the same cruise energy.

Reducing Visual Signature : Key Idea

The First Aircraft to Employ Active Visual Stealth Treatments -- the Grumman TBM Avenger, 1943

The concept of visual stealth has its roots in a 1943 U.S. Navy project codename Yehudi.[5,6] The intent of the program, which was highly secret at the time and came to light only in the 1980s, was to give Navy patrol aircraft a better chance of sinking enemy submarines. During 1942, German U-boats took a heavy toll on merchant marine shipping off the East Coast of the United States. Aircraft scrambled to attack the U-boats, but submarine captains called for crash dives whenever they spotted approaching attack planes. By the time an aircraft got close enough to sink a sub, it had disappeared. Yehudi's inventors needed a way to make the aircraft harder to see, and they realized that camouflage paint wouldn't do the job: Regardless of its color, the airplane would be a black dot against the sky. The only way to make the plane less visible was to light it up like a Christmas tree. The engineers fitted a TBM-3D Avenger torpedo-bomber with 10 sealed-beam lights, installed along the wing's leading edges and the rim of the engine cowling. When the intensity of the lights was adjusted to match the sky, the Avenger blended into the background. Tests proved that the Yehudi system lowered the visual acquisition range from 12 miles to two miles, allowing the Avenger to get within striking distance of its targets before they submerged.*

*R. Barrett and J. Melkert, *Proceedings of SPIE*, Vol. 5762, WA, 2005

An important question to address is how to reduce the visual signature of the aircraft. Even if the acoustic noise is reduced by using an electric motor and maintaining sufficient distance from the target, the aircraft can still be seen, negating the advantage offered by the quiet electric drive. The literature search revealed that visual signature reduction has been considered in the past. The idea is to illuminate the bottom of the aircraft, essentially hiding it by making the illumination of the aircraft match that of the sky.

Visual Signature Analysis: A specific Example*

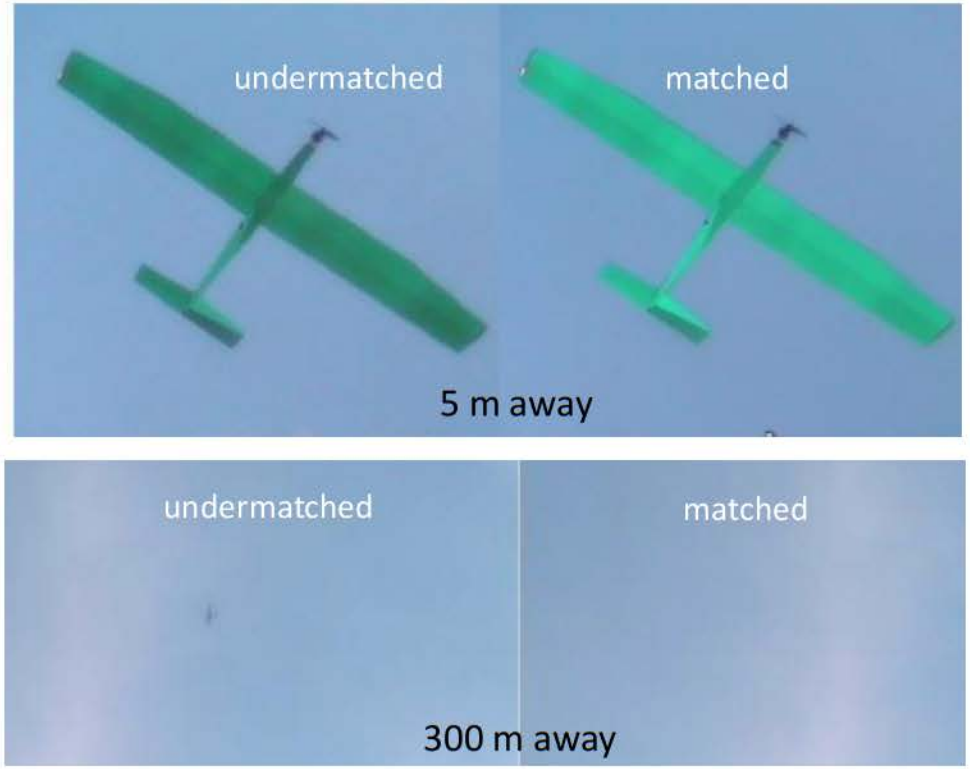

By varying radiating energy of electroluminescent sheets, the "visual cross-section" of an aircraft can be changed; appropriate illumination can make it disappear. How much power does that require?

*R. Barrett and J. Melkert, "UAV Visual Signature Suppression via Adaptive Materials, Smart Structures and Materials," *Proceedings of SPIE*, Vol. 5762, 2005, pp. 100-109

These figures give examples of what can be achieved by illuminating the bottom of the aircraft. When the illumination of the aircraft and that of sky is matched, the aircraft disappears. (The aircraft shown has 2 m wing span.) What is the trade-off between power needed to illuminate the aircraft surface, size of the aircraft, and reduction of its visual signature? The details of these calculations are given in Appendix A.

Hybrid-Electric UAV Design and Model Parameters

W = 6.6 kg - total weight; (2 kg battery weight /total weight = 0.3)
S - wing area (TBD) (m^2)
AR - wing aspect ratio (TBD)
e = 0.85 - Oswald efficiency factor
ρ = 1.06 kg/m^3 - air density
C_{d0} = 0.035 - zero lift drag coefficient
C_{lmax} = 1.25 - maximum lift coefficient
V_{cr} – cruise velocity (m/sec)
V_{st} – stall velocity (m/sec)
k – specific power required for visual signature reduction (W/m^2)
R – distance to target (m)
L_w – sound pressure level at 1 m (assumed) (dB)
L_p – Sound pressure level at R m (dB)
P_l – loiter power required (W)
P_r – cruise power required (W)

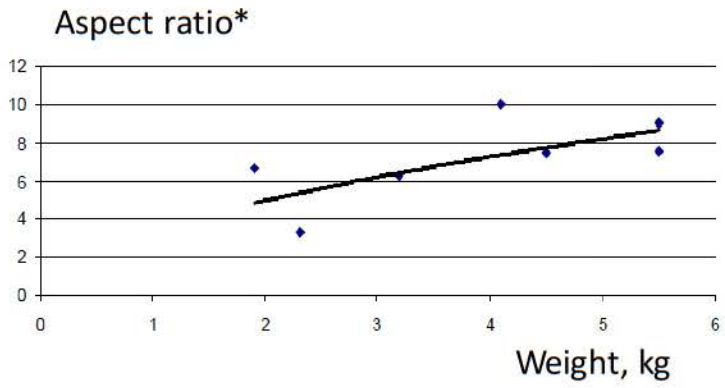

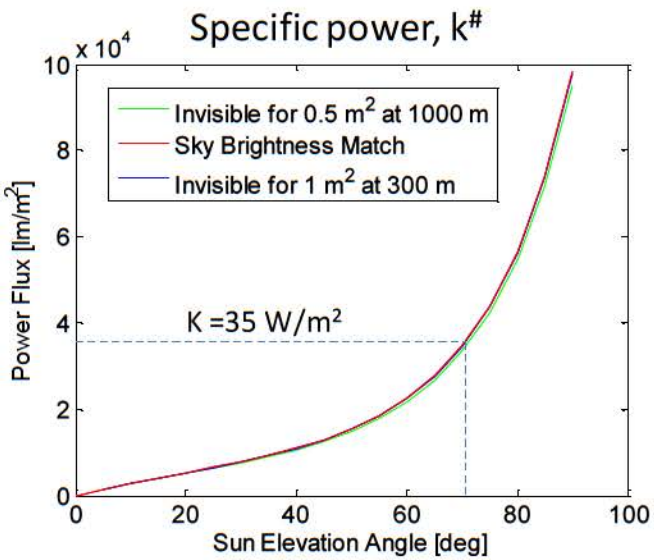

*G. Landolfo, PhD, University of Dayton, May 2008
#See Appendix A for details

Illuminating aircraft is power expensive. It turns out that at distances up to 1000 m, the power to illuminate the aircraft to match the sky intensity is a strong function of the sun elevation angle, but not of the distance to target or aircraft size. We choose a point on the plot at about 70° of sun elevation. At this point, the power to illuminate the aircraft is 35 W/m^2. As the sun elevates above that angle, the power required to match illumination of the sky steeply rises, making it more and more power expensive. Choosing 70° gives a reasonable compromise between relatively long invisibility window and relatively low power demands. It does mean, however, that if the aircraft is employed during the time of day when the sun has risen above 70°, the aircraft will be seen.

Another parameter that we choose for our conceptual design is the aircraft aspect ratio, AR. Larger AR values lead to more efficient loiter, but an increase in AR leads to heavier wings to counteract bending moments. We choose $AR = 9$, which is the number for Puma.

At this point, we have all the necessary input design parameters for the hybrid-electric UAV conceptual design: Total weigh is 6.6 kg, battery + propulsion + fuel weight is 2 kg, and power budget for visual signature reduction is 35 W/m^2.

Preliminary Design Flow Diagram

Input UAV Parameters
- HE UAV Weight, *W*
- Propulsion + battery + fuel weight
- *AR*
- Visual Signature Specific Power Required, *k*

Input desired loiter to cruise energy ratio

- *AR, S, $P_{cr}(V_{cr})$, P_l*
- *Loiter and cruise time*
- *Low acoustic signature distance to target*
- *IR Payload*

Choose infrared system

Optimize UAV design with respect to loiter power, P_l

$$P_l = W * \sqrt{\frac{2W}{\rho S}} * \frac{4C_{d0}}{[3C_d * \pi * e * AR]^{3/4}} + k * S$$

$$P_{cr} = \frac{1}{2} * \rho * {V_{cr}}^3 * W * C_{d0} * \frac{S}{W} + \frac{W}{\frac{1}{2} * \rho * \pi * e * AR} * \frac{W}{S}$$

$$\sqrt{AR} = \frac{2}{\rho} \sqrt{\frac{1}{3\pi C_{do}}} * \frac{W}{S} \frac{1}{V_{end}^2}$$

$$\frac{W}{S} = \frac{\rho * V_{stall}^2 C_{Lmax}}{2}$$

Choose IC/transmission | Choose Electric motor | Choose battery

Determine low acoustic signature distance

$$L_p = L_w - 10Log_{10}(2\pi R^2) - \alpha R$$

The conceptual design process is described on the diagram. The loiter power is calculated as a sum of two terms: power to overcome the drag force and power needed to illuminate the bottom of the aircraft. The wing area is then chosen to minimize the loiter power. With the wing area defined, cruise power as a function of cruise speed can be computed. There are two constraint equations that need to be satisfied: the endurance speed has to be greater than the stall speed by some safety margin, typically 3–5 m/s. Once the loiter and cruise power are determined, electric motor and internal-combustion engine/gearbox can be selected. The safe acoustic signature operating distance is determined via the noise-dissipation equation shown. The operating distance is used to select an infrared system with desired performance, given by the desired probability of identification.

Conceptual UAV Design and Performance

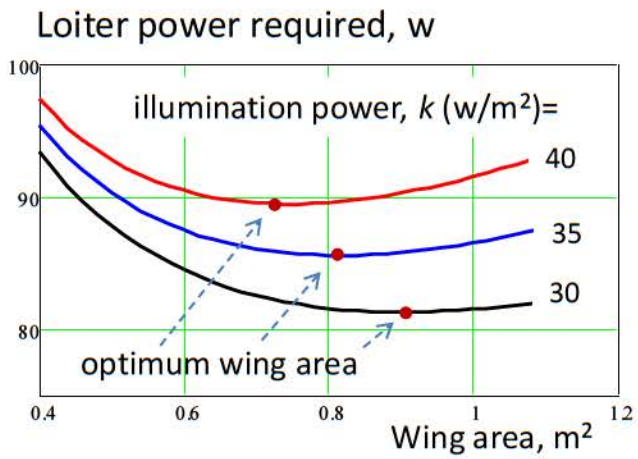

- Total UAV weight = 6.6 kg
- *AR* = 9 (Equal to Puma's value; larger *AR* is desired but it leads to increased wing weight, therefore it is treated as a constraint)
- Transmission efficiency: 0.8
- Propeller efficiency: 0.8
- Specific power for visual signature reduction* *k* = 30 - 40 W/m²

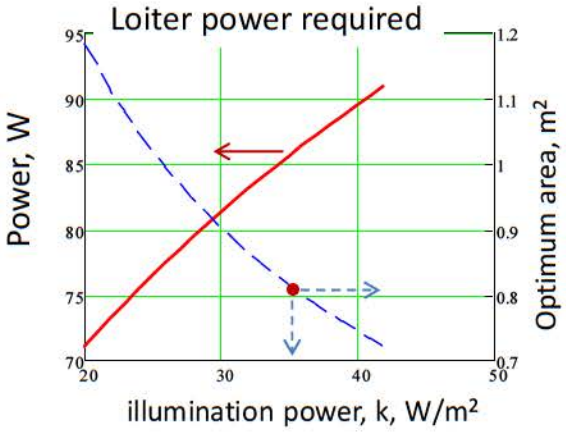

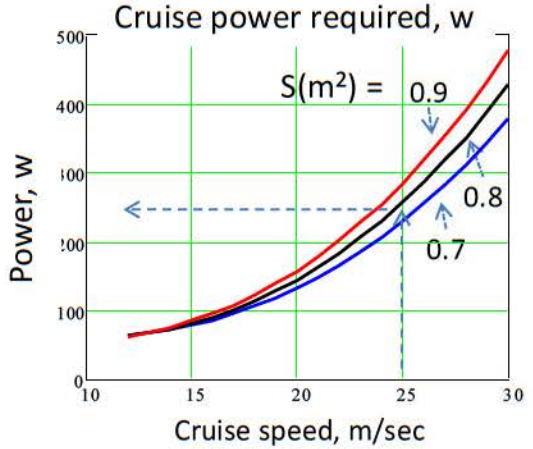

*At 35 w/m², the UAV will be invisible all year at 45 deg latitude and all fall and winter at 30 deg latitude; at 20 deg latitude it will be visible in the spring and summer for just under 3 hours a day around solar noon.

The slide presents an example of a conceptual design of a hybrid-electric UAV. With an illuminating power of 35 W/m^2 and the design parameters chosen, the loiter power required is minimized at the wing area of 0.81 m^2. The loiter power required is estimated to be 85 W. The cruise power at 25 m/sec is 250 W.

Choosing IC/Transmission and Electric Motor

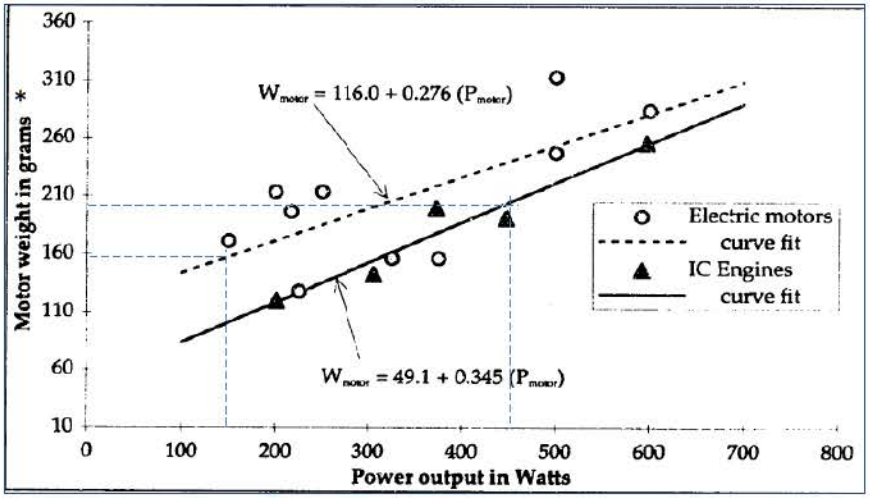

IC engine power

$$P_{ICE} = \frac{P_{cr}}{\eta_{tran} * \eta_{prop}} = \frac{250}{0.8 * 0.8} \sim 390\ w$$

Electric Motor Power

$$P_{EM} = \frac{P_l}{\eta_{tran} * \eta_{prop}} = \frac{85}{0.8 * 0.8} \sim 132\ w$$

IC energy efficiency

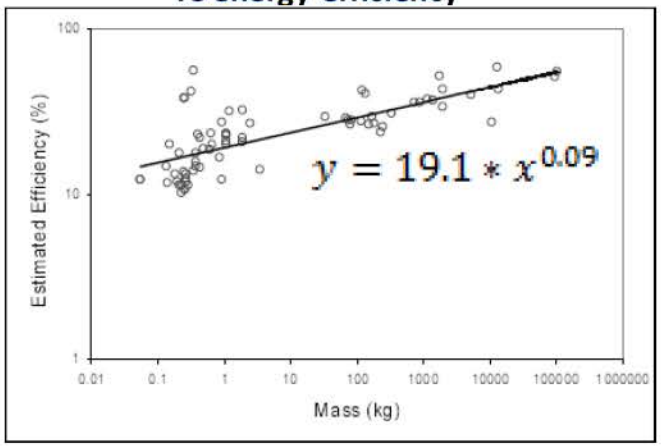

- *IC selection:*
  200 grams, η = 16%, 450 watts
  EM selection:
  160 grams, 150 watts
- *Gearbox weight = β*IC $_{weight}$*
  (β is between 1 and 2.5 of IC weight)
- *Battery + fuel weight:*
  [2 – IC $_{weight}$(1+β)]kg
- *Battery stored energy = 150 Wh/kg*

* A.M. Leon, "Preliminary Weight Sizing and Configuration Layout for a Small UAV," M.S. Thesis, MIT, 1997
S.K. Manon, "Performance Measurement and Scaling in Small ICE," M.S. Thesis, University of Maryland, 2006

The required internal-combustion engine and electric motor powers are calculated assuming 80% efficiency for the propeller and the gearbox transmission. We select a 450 W internal-combustion engine weighing 200 g and a 150 W electric motor weighing 160 g. The efficiency of the internal-combustion engine is estimated to be 16% via equation shown.

Safe Distance to Target for Acoustic Signature Reduction

How quiet does the UAV have to be?

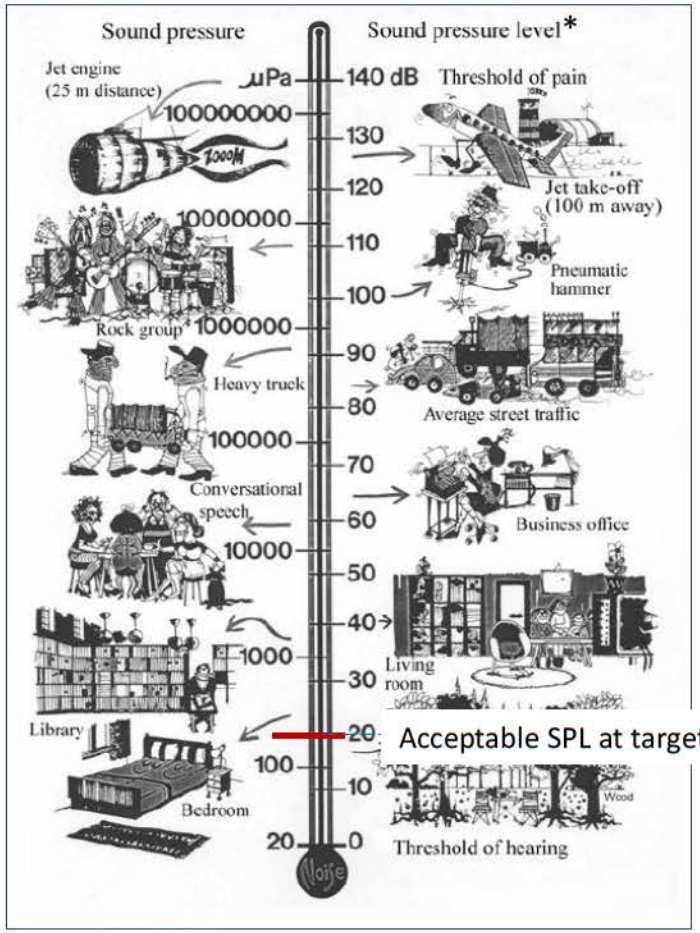

*A. L. Rogers, "Wind Turbine Acoustic Noise," R ER Laboratory Report, University of Massachusetts at Amherst, 2002

$$SPL = SPL_o - 10\log(2\pi R^2) - \alpha R^*$$

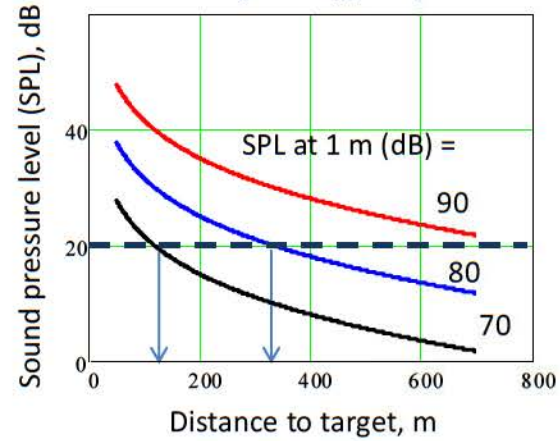

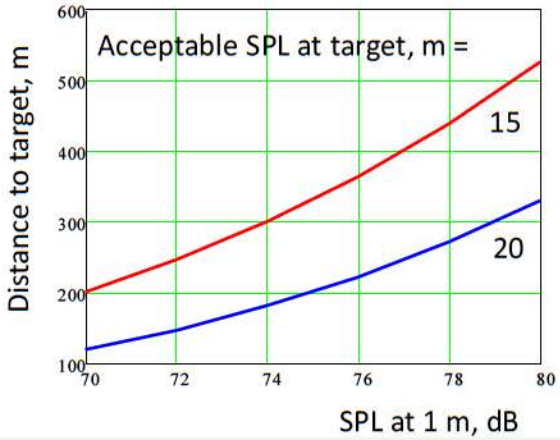

With the SPL between 70 and 80 dB at 1 m (current EM UAV noise levels), the UAV will have to be 120 - 320 m from target to maintain at most 20 dB at target

The "safe" operating distance clearly depends on the maximum allowable noise level at target. We use the equation shown to estimate the power dissipation as a function of distance (with the atmospheric attenuation coefficient of 0.05). The SPL at 1 m as a function of motor power and propeller size for this class of UAV is unknown. We found some experimental values for a mini UAV to be in the range of 70 dB (Leslie, at al, "Broadband Noise Reduction from a Mini – UAV Propeller through Boundary Layer Tripping," *Acoustics 2008*, Geelong, Victoria, Australia, November 2008). To err on the conservative side, we take the sound pressure level (SPL) at 1 m to be 80 dB. With these values, for a 20 dB maximum allowable SPL at the target, we estimate the safe operating distance to be about 300–350 m.

IR Camera Design Specifications

Primary Design Requirements: Night Vision, Lightweight (< 500g), Low Power

Best option seems to be a SWIR camera based on InGaAs, sensitive from 0.9-1.7 µm:

- SWIR > Vis/NIR
  - Need signal photons
  - Starlight provides sufficient illumination for short-range SWIR surveillance
- SWIR > MWIR/LWIR
  - Better resolution at lower wavelengths
  - Cooling unnecessary
  - Reflected-Light imagery less susceptible to contrast reversal/crossover periods

Considered two small COTS SWIR camera modules:

Goodrich Corp: 1280J-15A	(*highest resolution and sensitivity*)
FLIR Systems Inc.: Tau SWIR	(*smaller, lighter*)

Considered two options for optical materials for each camera lens:

Glass	(*better transmission in SWIR*)
Plastic (PMMA)	(*lighter weight*)

Estimated weight of each full sensor system (camera + lens + housing):

1280J-15A w/ glass lens:	535 g (this one was not estimated but pulled directly from spec sheets)
1280J-15A w/ plastic lens:	430 g
Tau SWIR w/ glass lens:	260 g
Tau SWIR w/ plastic lens:	200 g

IR Camera Performance Model Description

Investigated performance for the four camera designs with SSCamIP

SSCamIP:#

- The predominant accredited target acquisition model for reflected light imaging sensors
- Developed, validated, and verified by U.S. Army NVESD*
- Range-performance predictions are empirical (based on forced-choice experiments)
- Methodology:
  - Model is based on the Targeting Task Performance (TTP) metric
    - Sensor capabilities are encapsulated by Contrast Threshold Function (CTF)
    - CTF + Scenario → TTP Metric (target- and scenario-specific image quality)
    - TTP Metric → Probability of Task Accomplishment
- Inputs
  - Sensor specifications (optics / detector / etc.)
  - Scenario details (target / illumination source / etc.)
- Outputs
  - Probability of target detection/recognition/identification

See Appendix B for details

* U.S. Army Night Vision and Electronic Sensors Directorate (NVESD.)

R.H. Vollmerhausen, E. Jacobs, J. Hixson, and M. Friedman, "The Targeting Task Performance (TTP) Metric: A New Model for Predicting Target Acquisition Performance." U.S. Army RDECOM, CERDEC, Technical Report AMSEL-NV-TR-230, January 2006.

What is the IR performance vs. Payload Weight Trade-off at 300 – 400 m?

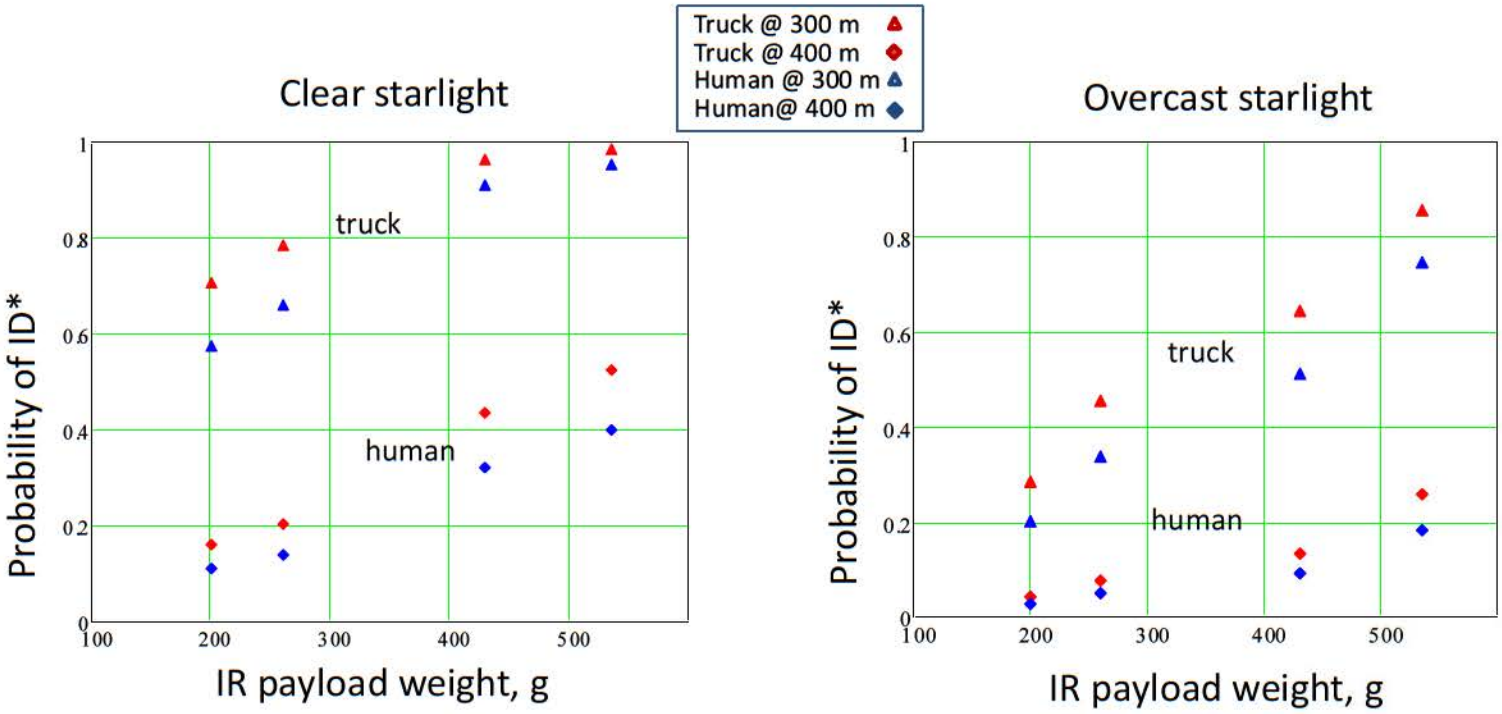

The IR payload of 500 g (~1.1 lb) seems to be sufficient for a reasonable performance at night at the distance of interest. The trade-off analysis between low acoustic signature operating distance, noise level , and payload weight can be performed if more accurate noise levels are known.

* The analysis is based on SSCamIP model, U.S. Army Night Vision and Electronic Sensors Directorate (NVESD); see Appendix A for details.

As can be seen from the slide, for operating distance of 300–400 m, the IR camera weighing 0.5 kg delivers a very good performance for a truck: almost 100% probability of identification (PID). Identification performance is significantly reduced when the target is a human. While we have no specific target acquisition performance requirements for this sensor against humans, we suggest that this approach can be used to determine a necessary sensor payload if such requirements are specified.

Conceptual Design Specifications of Hybrid-Electric UAV

- UAV weight: 6.6 kg (14.5 lb)
- IC: 200 grams, 450 watts
- Gearbox weight ($\beta = 2$): 400 grams
- Electric Motor : 160 grams, 150 watts
- Wing surface area: 0.81 m^2
- Wing Aspect Ratio: 9
- IR Payload weight: 0.5 kg (1.1 lb)

Hybrid-Electric UAV Battery weight (150 Wh/kg):
- Design #1: 1.2 kg
- Design #2: 1.1 kg
- Design #3: 1.0 kg

The available loiter energy can be traded with that of internal-combustion powered cruise: decreasing loiter by 1 Wh leads to ~13.3 Wh increase in cruise. *The advantage of such a hybrid-electric UAV design depends on needs of a particular mission.*

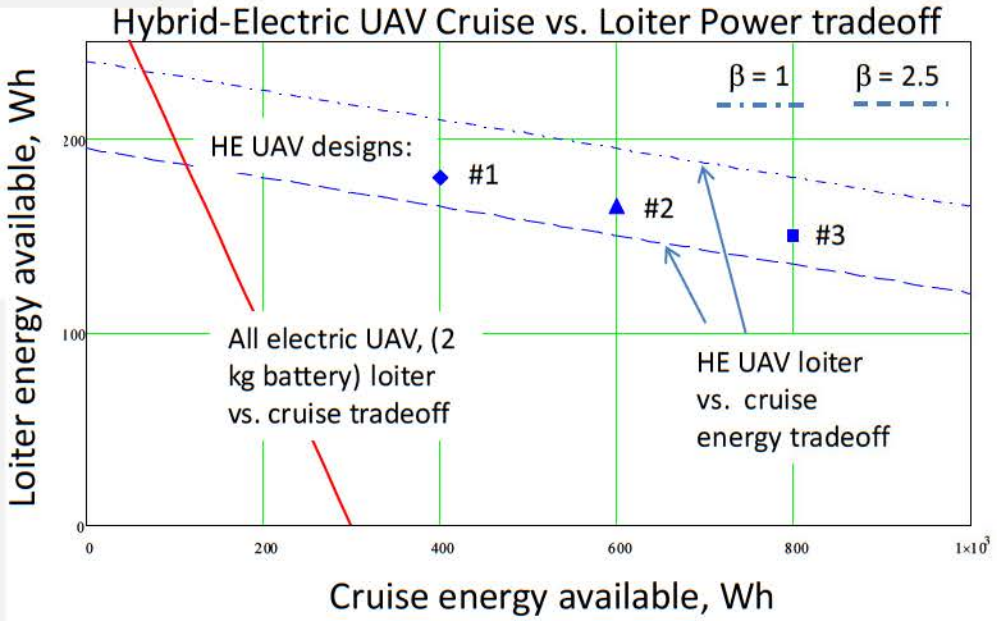

Our conceptual design resulted in a hybrid-electric UAV with the specifications shown. We assumed a conservative gearbox design with a weight of twice of that of the internal-combustion engine. The wing aspect ratio is equal to that of Puma, and the wing area is 0.81 m^2, just under that of the Puma ($0.832m^2$). To demonstrate loiter vs. cruise energy trade-offs, we consider three different electric battery weight options: 1.2, 1.1, and 1.0 kg. As the battery weight decreases, more fuel can be taken on board, and the cruise energy increases, as is shown by points #1, #2, and #3 on the figure.

The conceptual design shown, while most likely not optimum, demonstrates that an extended cruise endurance hybrid-electric UAV is feasible. The cruise extension, however, comes at the expense of reducing the (quiet) electric energy available. The trade-off appears to be advantageous in the favor of the cruise range extension: for every 1 Wh loss of the electric energy, 13.3 Wh of cruise energy is gained. The design utilized existing electric motor, battery, and internal-combustion engine specifications. The only component that needs to be better defined is the gearbox.

The conceptual design includes estimates of the power needed to illuminate the bottom of the aircraft to render it invisible in the sky. To our knowledge, these calculations are not available in the open literature, and are the most important original contribution of this work.

Conclusions

Conceptual design of a hybrid-electric UAV demonstrates that an extended cruise endurance hybrid-electric UAV is feasible. The cruise extension, however, comes at the expense of reducing the electric energy on board: for every 1 Wh loss of electric energy for loiter, 13.3 Wh of cruise energy is gained.

Visual signature can be reduced by illuminating the hybrid-electric UAV's bottom surface; a model for estimating power cost associated with the signature reduction is developed and can be used to determine illuminating power level and position of the aircraft with respect to sun location to render it invisible.

Acoustic signature can be reduced by maintaining a minimum distance to target, which (for the designed hybrid-electric UAV) is estimated to be 300 – 400 m; more accurate estimates are desired, but are outside the scope of this analysis.

An IR system, estimated at 0.5 kg as a part of the designed hybrid-electric UAV payload, can be used to identify a person or truck at 350 m in clear starlight with 0.5 and 0.95 probability, respectively.

All hybrid-electric UAV parts, with the exception of gearbox, are commercially available. The gearbox design, including minimizing its weight, requires further development.

Appendix A
Estimating Illuminating Power for Visual Signature Reduction

Jeremy Teichman

Illuminance: Background and Definitions

- Luminous intensity I: Visible light emitted per solid angle (candela (cd) or lumens/steradian (lm/sr))
- Luminous power P: Total visible light emitted (lm)
- Illuminance E: At a distance D, the flux of visible light per unit area is I/D^2 (lx or lm/m^2)
- Luminance L: Brightness (cd/m^2 or lm/m^2/sr) – luminous intensity per unit source area or equivalently illuminance per solid angle of source
  - For a resolved object, luminance is invariant with distance because the solid angle subtended grows as quickly as the illuminance. If the object appears as a point source, luminance will vary as $1/D^2$.

For monochromatic light at 555 nm, 682 lumens = 1 watt

These definitions[2] set the stage for a discussion of visible light energy reaching an observer on the ground. The brightness or luminance becomes important in discussions of visibility on subsequent charts. Due to spreading of the light, illuminance is inversely proportional to the square of the distance from the source $E = I_0/D^2$,[3] where E is the received illuminance, and I_0 is the luminous intensity of the source. In addition, a scattering and/or absorbing medium, such as the atmosphere, will attenuate light according to Lambert's law, which describes exponential attenuation: $E = E_0 e^{-aD}$, where E_0 is the original illuminance, a is the attenuation coefficient, and D is the distance traveled. When viewing through the atmosphere, the viewing elevation angle contributes to the attenuation because the amount of air traversed by the line of sight varies with elevation angle. The attenuation coefficient at 550 nm is $a = 2.0 \times 10^{-5}$ m^{-1} at sea level. The attenuation along a path through the atmosphere is based on the distance at sea level required to traverse an equivalent mass of air to that along the true path. The air mass traversed looking out beyond the atmosphere at the horizon is 38 times that looking at zenith.[4] For an exponential atmosphere, a good approximation, even near the horizon, is $\frac{m}{m_0} = \sqrt{\frac{\pi R_E}{2H}}\left[e^{\frac{R_E \sin^2\theta}{2H}} \operatorname{erfc}\left(\frac{\sqrt{R_E}\sin\theta}{\sqrt{2H}} \right) - e^{-\frac{D}{2R_E H}\left(\sqrt{(z+R_E)^2 - R_E^2\cos^2\theta} + R_E\sin\theta\right)} e^{\frac{(z+R_E)^2 - R_E^2\cos^2\theta}{2R_E H}} \operatorname{erfc}\left(\sqrt{\frac{(z+R_E)^2 - R_E^2\cos^2\theta}{2R_E H}} \right) \right]$ where R_E is the radius of the earth, H is the atmospheric scale height, D is the distance to the object, z is the altitude of the object, θ is the elevation angle, m is the air mass, and m_0 is the zenith air mass. The total illuminance is given by $E = \frac{I_0}{D^2} e^{-a\frac{m}{m_0}H}$ also known as Allard's law.[5]

[2] e.g. Earle B. Brown, *Modern Optics*, New York: Reinhold Publishing corporation, 1965.

[3] L. Dunkelman and R. Scolnik, "Solar Spectral Irradiance and Vertical Atmospheric Attenuation in the Visible and Ultraviolet," *Journal of the Optical Society of America*, Vol. 49, No. 4, 1959.

[4] F. Kasten and A. T. Young, "Revised optical air mass tables and approximation formula," *Applied Optics*, Vol. 28, No. 22, 1989.

[5] Edward Friedman and John Lester Miller, *Photonics rules of thumb: optics, electro-optics, fiber optics, and lasers*, p48.

Visibility

- Visibility depends on:
  - Ambient light adaptation level – background luminance ($W/m^2/sr$)
    - Starlight = $5x10^{-7}$ $W/m^2/ster$, Daylight = 5 $W/m^2/sr$
    - Bright light viewing uses cones, low light uses rods.
      - Rods are single photon sensitive.
      - Bright light sensitivity is principally central vision.
      - Low light sensitivity is highly peripheral.
  - Size (sr)
    - Critical visual angle
      - Angular width of largest apparent point source
        - » Starlight = 2 mrad
        - » Daylight = 0.2 mrad
  - Contrast = $(L\text{-}L_B)/L_B$
    - L_B = Background luminance
    - Ranges from -1 to +∞
    - Minimum contrast:
      - Starlight = 710
      - Daylight = 0.4

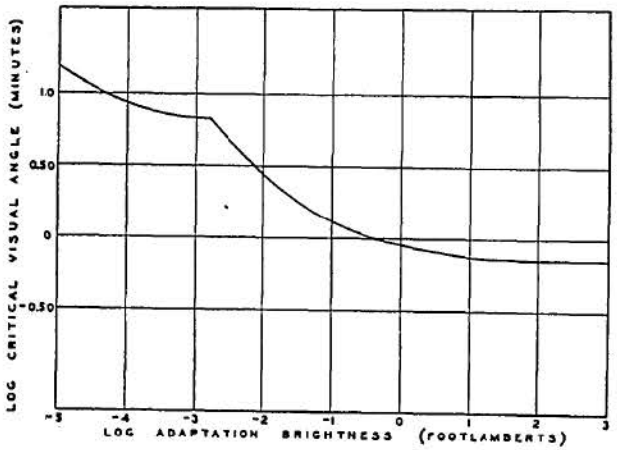

Critical Visual Angle as Function of Adaptation Brightness
H. Richard Blackwell, Contrast Threshold of the Human Eye,
Journal of the Optical Society of America, Vol. 36 No. 11, Nov. 1946.

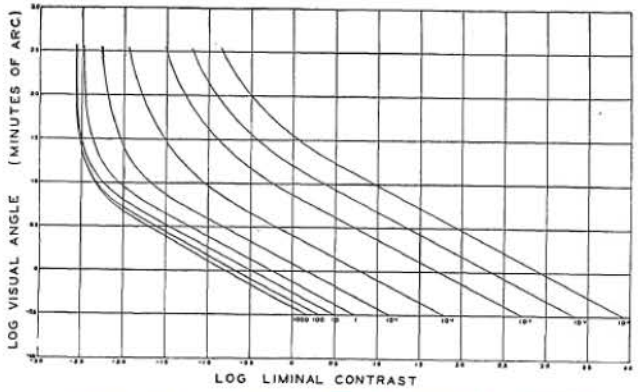

H. Richard Blackwell, Contrast Threshold of the Human Eye,
Journal of the Optical Society of America, Vol. 36 No. 11, Nov. 1946.

Luminance is invariant with distance because as the illuminance drops with the distance squared, the solid angle subtended by the source varies inversely with the distance squared. However, if the source is sufficiently distant that it appears as a point source (really the minimum resolvable size), the illuminance continues to drop with the distance squared, but the apparent size remains constant, causing the apparent luminance to drop as $1/D^2$. Thus apparent luminance is given by $L = \frac{E}{\max(\Omega, \Omega_{min})}$ where Ω is the solid angle subtended by the source and Ω_{min} is the minimum resolvable solid angle.

Luminance of the path between the observer and the object also tends to diminish contrast. Scattering of ambient light off molecules in the path generates path luminance. The combined effects of attenuation and path luminance lead to apparent luminance of an object asymptotically approaching background luminance as the intervening material (atmosphere traversed) increases $L = \left[\frac{I_0}{D^2 \Omega} e^{-a\frac{m}{m_0}H} + L_B \left(1 - e^{-a\frac{m}{m_0}H} \right) \right] \frac{\Omega}{\max(\Omega, \Omega_{min})}$ where the second term in the brackets represents the path luminance (L_0 is the background luminance).

The most basic determinant of whether an object is detectable by the unaided eye is its contrast with the background. Contrast is defined as the excess brightness of the object relative to the background $(L\text{-}L_B)/L_B$, where L is the apparent object luminance, and L_B is the background luminance. An object brighter than the background presents positive contrast, and an object darker than the background presents negative contrast. An object cannot have negative luminance, so contrast ranges from negative one to infinity. The absolute value of contrast determines visibility, so negative and positive contrasts of the same magnitude contribute equally to visibility.[6]

The size of an object (angle subtended) also contributes to its visibility, with larger objects being more visible. Below a critical angular size, the objects appear as point sources, and the size does not contribute directly. However, the absolute contrast requirement continues to vary because the apparent luminance diverges from the absolute luminance.[7] In this regime of apparent point sources, the threshold represents a constant minimally perceptible illuminance difference.

The third variable contributing to human visibility thresholds is ambient light level. The detector in the human eye, the retina, contains two types of light sensors, rods and cones. The rods, which are far more sensitive than the cones, are principally used for

[6] J. Gordon, "Visibility: Optical Properties of Objects and Backgrounds," *Applied Optics*, Vol. 3, No. 5, 1964.

[7] H. R. Blackwell, "Contrast Thresholds of the Human Eye," *Journal of the Optical Society of America*, Vol. 36, No. 11, 1946.

vision in dim lighting and the cones for bright environments. The rods and the cones are distributed differently over the retina, and neither is distributed homogeneously. Because the eye adapts to the ambient light level and the dominant modes of vision vary with the adaptation light level, human thresholds for discerning objects also depend on the ambient light adaptation level. Greater contrast is required at lower ambient light levels. The critical angular size below which objects appear as point sources also grows with lower ambient light levels. The graph above shows the threshold contrast level as a function of object size and ambient light level.

Invisibility by Contrast Reduction

- Active illumination of an object darker than the background can reduce contrast and prevent visual detection.
- For an airborne object, attenuation and path luminance are both minimized at nadir, so barring directional variation in background luminance, it is most visible from nadir.
- The amount of lighting required to achieve contrast invisibility will depend on object size, distance, and ambient lighting.

$$L_0^* = L_B\left(1 - C_t\left(\Omega, L_B\right)e^{aH\frac{m(D,\theta)}{m_0}}\right)$$

The contrast presented by a body whose luminance at zero distance is L_0 is

$$C = \frac{L - L_B}{L_B} = \left[\frac{I_0}{L_B D^2 \Omega} - 1 \right] e^{-a\frac{m}{m_0}H} = \left[\frac{I_0}{L_B A} - 1 \right] e^{-a\frac{m}{m_0}H} = \left[\frac{L_0}{L_B} - 1 \right] e^{-a\frac{m}{m_0}H} .$$

For a contrast threshold $C_t(\Omega,L_B)$ and a darker-than-background object, the threshold luminance for invisibility is given by

$$L_0^* = L_B \left(1 - C_t e^{a\frac{m}{m_0}H} \right)$$

for $C_t e^{a\frac{m}{m_0}H} < 1$ (otherwise, even a perfectly black object would be invisible).

Required Luminance for Vanishing

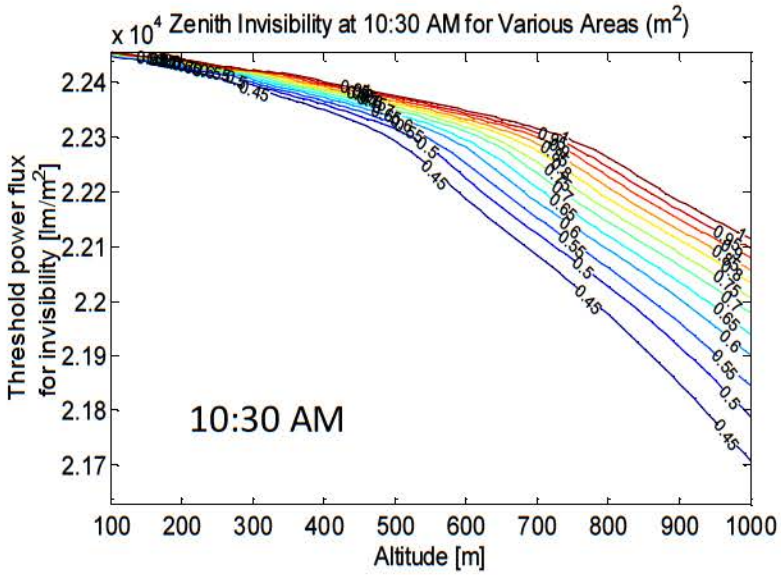

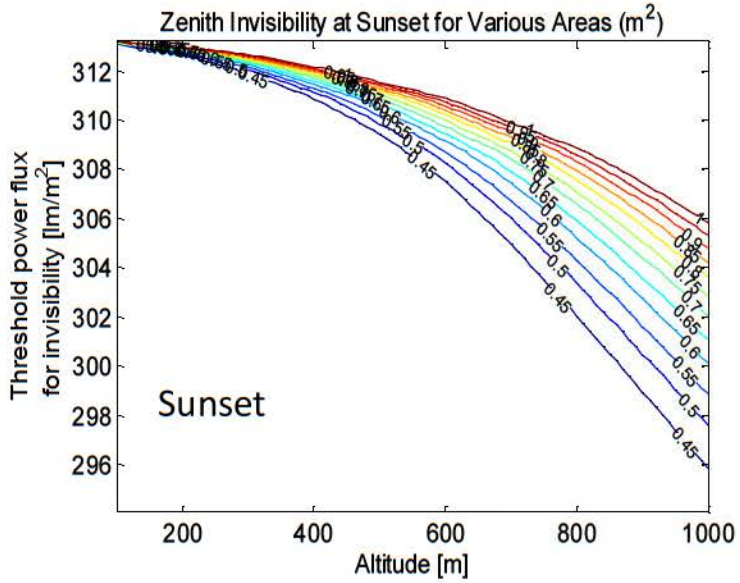

- Each curve represents a projected area. Curves range from 0.45 m^2 to 1 m^2.
- X-axis represents altitude from 100 to 1000 m.
- Y-axis represents necessary visible power flux. For daytime operation the brightness required by the active illumination differs from the background sky luminance by less than 10% over the full range of parameters considered.
- **For this parameter neighborhood, an object needs to nearly match sky luminance to disappear.**

At 10% lighting efficiency, 10:30 AM: 330 W/m^2, sunset: 4.6 W/m^2

Time of Day Effect

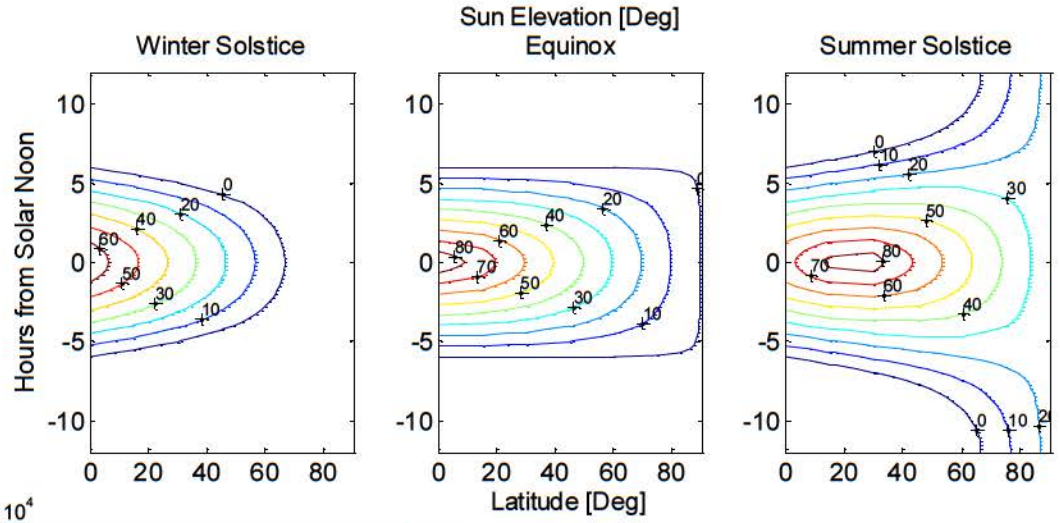

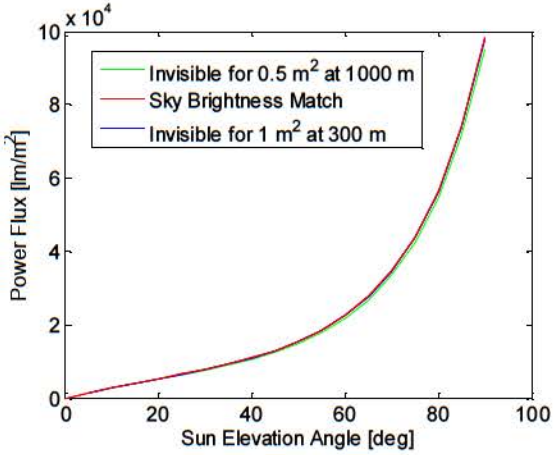

Sky brightness matching must be achieved within 4% for daytime clear sky for altitudes up to 1000 m and areas down to 0.5 m^2.

Time of Day Effect Example

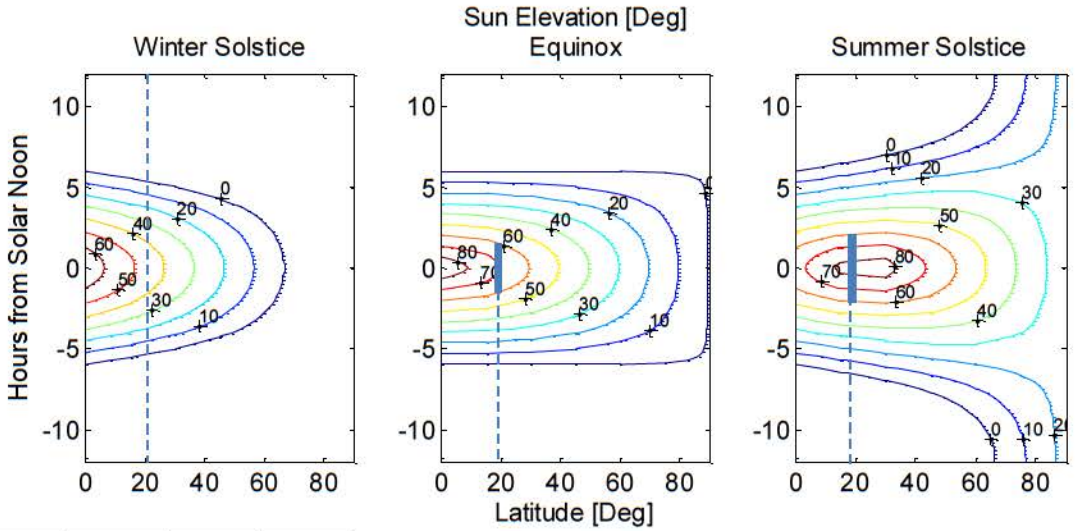

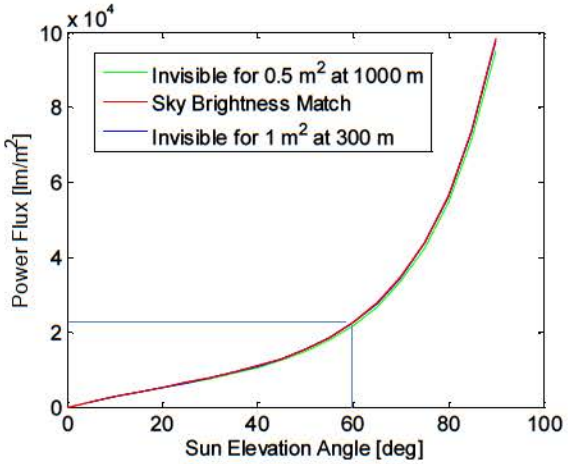

Note that a 22,000 lux 1 m^2 object will be invisible all year at 45 deg latitude and all fall and winter at 30 deg latitude, but at 20 deg latitude it will be visible in the spring and summer for about 3 hours a day around solar noon.

Appendix B

INTRODUCTION

SSCamIP, developed by the U.S. Army Night Vision and Electronic Sensors Directorate (NVESD), is PC-based software, developed in MATLAB, that models change-coupled displays (CCDs) and other cameras with staring arrays of detectors that sense reflected radiation in the 0.4-2 μm spectral band.[1]

The model predicts the contrast threshold function (CTF) for a human observing a scene with such an imager. Using the MRC, SSCamIP employs NVESD's targeting task performance (TTP) metric[2] as a criterion to predict the target-acquisition-range performance achievable when using the sensor.

GENERAL DESCRIPTION AND EVOLUTION OF MODEL:

SSCamIP is the 2006 version of the NVESD reflected-light imaging model. Earlier examples (e.g., FLIR92 and Acquire) provided target-acquisition-performance estimates for first- and second-generation thermal scanning sensors.[3] NVTherm 2002 extended these models to provide performance estimates for thermal staring imagers, and SSCam 2002 was developed to extend these concepts to reflected-light imagery.[4] Two characteristics of staring sensors required significant revisions of the earlier models. First, due to the high contrast sensitivity of many staring devices, it can be important to consider the limitations of the human eye when modeling target-acquisition performance. Second, in staring sensors, the limitations on detector size, spacing, and fill factor result in under-sampled imagery. The resultant sampling artifacts can affect imager performance. The eye-contrast effect was modeled in

---

[1] Night Vision and Electronic Sensors Directorate, "Night Vision Solid State Camera and Image Processing Performance Model: User's Manual & Reference Guide"

[2] R.H. Vollmerhausen, E. Jacobs, J. Hixson, and M. Friedman, "The Targeting Task Performance (TTP) Metric: A New Model for Predicting Target Acquisition Performance". U.S. Army RDECOM, CERDEC, Technical Report AMSEL-NV-TR-230, January 2006.

[3] J. Howe, "Electro-Optical Imaging System Performance Prediction," in Electro-Optical Systems Design, Analysis, and Testing, (Dudzik ed.), The Infrared and Electro-Optical Systems Handbook, Vol. 4, p. 92, ERIM IIAC, Ann Arbor, MI and SPIE, Bellingham, WA.

[4] T. Maurer, R.G. Driggers, R. Vollmerhausen, and M. Friedman, "2002 NVTherm Improvements", *Proceedings of SPIE* Vol. 4719 (2002), pp. 15-23.

SSCam 2002 by quadratically adding visual noise to the sensor noise in the minimum resolvable contrast (MRC) equation. Sampling issues were addressed by assuming an increase in the system's blur or, equivalently, a contraction in the system's modulation transfer function (MTF). The 2002 sampling treatment was devised to fit empirical results; it was not grounded in theory. Target acquisition was predicted using Johnson criteria (1958),[5] wherein the MRC curve was used to map the scene contrast to a maximum resolvable spatial frequency. The number of resolvable frequency cycles across the target dimension was compared to N_{50}, the empirically derived number of cycles necessary for 50% probability of target acquisition (either detection, recognition, or identification).

SSCam 2002

The following list is a description of the method used by SSCam 2002:

1. Determine the range to the target and the zero-range modulation contrast ΔC_0 between target and background. Zero-range modulation contrast is defined as

$$\Delta C_0 = \frac{|\rho_T - \rho_B|}{\rho_T + \rho_B},$$

where ρ_T is the average target reflectance across the appropriately weighted spectral band, and ρ_B is the background reflectance. Given the effective atmospheric attenuation (τA) in the imager's spectral band as a function of range, we can calculate the apparent ΔC of the target at the given range:

$$\Delta C_{app} = \Delta C_0 * \tau_A$$

2. Calculate the system's MRC. The MRC depends on the camera's angular resolution and low-light sensitivity; these are functions of the optical and detector devices as well as the signal processing and display used. MRC expresses the minimum resolvable contrast as a function of object component spatial frequency. We can use the inverse function of the MRC curve to determine the maximum resolvable spatial frequency $\xi_{\max}$ of the sensor given the apparent ΔC:

$$\Delta C_{app} = \mathrm{MRC}(\xi_{\max})$$

$$\xi_{\max} = \mathrm{MRC}^{-1}(\Delta C_{app})$$

[5] J. Johnson, "Analysis of Imaging Forming Systems", *Proceedings of the Image Intensifier Symposium*, Oct. 6-7, 1958.

3. Determine the target's critical dimension H_{Targ}. This is usually the square root of the target cross-sectional area, as viewed from the imager position. Then for a given range to target R, calculate the maximum number of resolvable cycles N across the target dimension, using the expression

$$N = \frac{\xi_{\max} H_{\text{Targ}}}{R}$$

4. Determine the probability of detection, recognition, and/or identification using the target transfer probability function (TTPF)

$$P = \frac{\left({}^{N}/_{N_{50}}\right)^{E}}{\left(1 + \left({}^{N}/_{N_{50}}\right)\right)^{E}}$$

In the above equation, $E = 2.7 + 0.7({}^{N}/_{N_{50}})$, where N_{50} is the number of cycles on target required for 50% probability of task accomplishment; it is therefore a quantification of the task difficulty. Values for N_{50} and the expression for E are derived from empirical experimental evidence.

As is evident from the above methodology, the capabilities of the sensor itself, as represented in the model, are entirely summarized by the MRC. No sensor-specific information is used in steps 1, 3, or 4. Also, the MRC contains no explicit dependence on the target, the atmosphere or any other scenario phenomenology. Step 2 of the above methodology, the MRC calculation, depends only on technical information specific to the sensor; it represents this information in a single curve. The other steps illustrated above depend only on the details of the scenario, not on the sensor. Thus, the MRC is a scenario-independent sensor metric; it is used in conjunction with scenario information to determine range performance.

SSCamIP

SSCamIP (2006) modified the above process. The primary shortcoming of the 2002 version was that the performance predictions ignored the shape of the MRC; they depended on only the value of the inverse function at a single contrast. Subsequent experiments showed that the shape of the full MRC curve could be used to improve performance predictions.

For the 2006 version, MRC was replaced by a similar, but differently derived, metric: contrast threshold function (CTF). For a given light level, the CTF is the threshold modulation contrast perceivable by the human eye as a function of spatial frequency. While this concept does not involve artificial sensors, SSCamIP uses existing CTF data and combines those data with sensor information (optical and detector device specifications, signal processing, display fidelity) to express the CTF as a function, in object space, for the scene being viewed through the imager. From the CTF and the apparent modulation contrast ΔC_{app}, SSCamIP computes the TTP metric by integrating the square root of the excess contrast over the resolvable spatial frequencies.

The following list describes the method used by SSCamIP:

1. Determine the range to the target and the zero-range modulation contrast, ΔC_0, between target and background. Zero-range modulation contrast is defined as

$$\Delta C_0 = \frac{|\rho_T - \rho_B|}{\rho_T + \rho_B},$$

   where ρ_T is the average target reflectance across the appropriately weighted spectral band, and ρ_B is the background reflectance. Given the effective atmospheric attenuation (τ_A) in the imager's spectral band as a function of range, we can calculate the apparent ΔC of the target at the given range:

$$\Delta C_{app} = \Delta C_0 * \tau_A$$

2. Calculate the system's CTF, called $\mathrm{CTF_{sys}}$. The $\mathrm{CTF_{sys}}$ depends on the camera's angular resolution and low-light sensitivity; these are functions of the optical and detector devices as well as the signal processing and display used. $\mathrm{CTF_{sys}}$ expresses the threshold (i.e., barely discernible) contrast as a function of object component spatial frequency.
3. From the apparent ΔC (step 1, above) and the $\mathrm{CTF_{sys}}$ curve, we can compute the TTP metric value:

$$\mathrm{TTP} = \int_{\{\xi | \Delta C_{app} > \mathrm{CTF_{sys}}(\xi)\}} \left[\frac{\Delta C_{app}}{\mathrm{CTF_{sys}}(\xi)}\right]^{1/2} d\xi$$

4. Determine the target's critical dimension H_{Targ}. This is usually the square root of the target cross-sectional area, as viewed from the imager position. Then for a given range to target R, calculate the maximum number of TTP-weighted cycles V across the target dimension, using the expression

$$V = \frac{(\mathrm{TTP})(H_{\mathrm{Targ}})}{R}$$

5. Determine the probability of detection, recognition, and/or identification using the target transfer probability function (TTPF):

$$P = \frac{\left({}^{V}/_{V_{50}}\right)^{E}}{\left(1 + \left({}^{V}/_{V_{50}}\right)\right)^{E}}$$

In the above equation, $E = 1.51 + 0.24({}^{V}/_{V_{50}})$, where V_{50} is the metric value required for 50% probability of task accomplishment; it is therefore a quantification of the task difficulty. Values for V_{50} and the expression for E are derived from empirical experimental evidence.

COMPARISON with FIELDED SYSTEMS

Figure 2 shows the relationship between SSCamIP, laboratory measurements, and field performance. The model predicts the minimum resolvable contrast (MRC) perceivable given the sensor and display design. This can be verified by laboratory measurement. The model also predicts the target-acquisition performance that is achievable if the sensor meets its design expectations. These field predictions are based on a long history of both field and laboratory experiments carried out by the U.S. Army Night Vision and Electronic Sensors Directorate (NVESD) that relate the MRC to field performance.

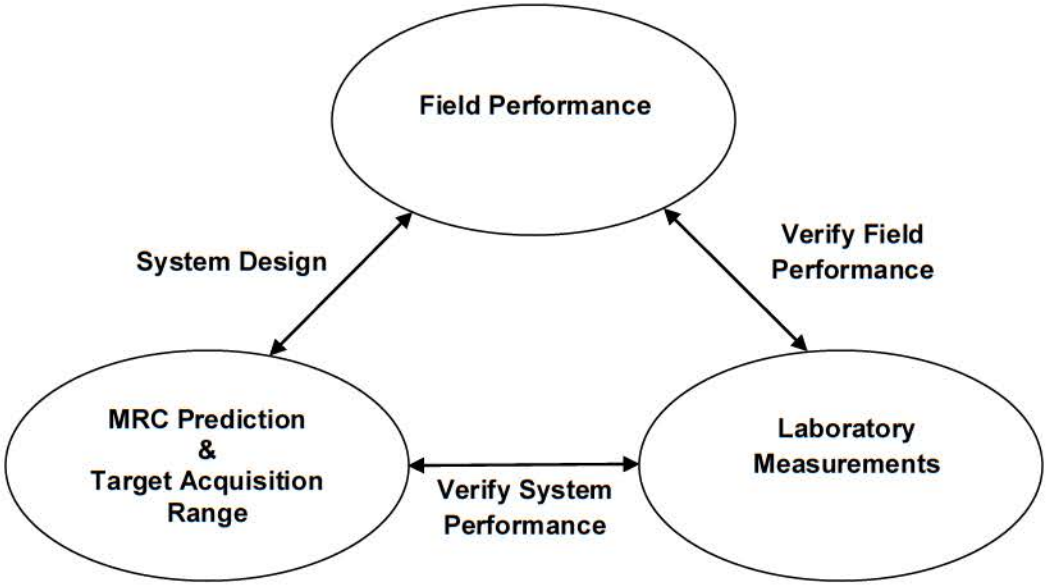

Figure 2: SSCamIP predicts the MRC, which is measurable in the lab, and the target-acquisition performance, which is achievable in the field.

Range predictions are most accurate when comparing two sensors or sensor designs. However, SSCamIP can also predict *absolute* range performance, provided the user can adequately specify the difficulty of the task in terms of a V_{50} value, the number of resolvable cycles on a target necessary for a 50% probability of accomplishing the task. NVESD has performed experiments to empirically estimate appropriate values for V_{50} across various target sets. NVESD has estimated values for V_{50} for three tasks: target detection, recognition, and identification. This analysis only considers identification. While the NVESD results do show some dependence on the set of targets and confusers chosen for a particular experiment, our model uses a single V_{50} across the scenarios for our identification task. The V_{50} value we have selected is a "typical" value for target identification recommended by NVESD after its experiments.

MODEL ASSUMPTIONS

In the NVESD imaging models, sensors are analyzed in the vertical and horizontal directions separately, and an overall performance is calculated from the separate analyses. The point spread function (PSF) and the associated modulation transfer function (MTF) are assumed to be separable, which reduces the analysis to one dimension. The separability assumptions are almost never completely satisfied, but there is usually only a small error (~3%) associated with assuming separability.

SSCamIP also assumes that these systems are shift invariant, so that the system's PSF does not change significantly from point to point in the image. By assuming that MTFs are real-valued, modeled system PSF is restricted to symmetrical blur. For both of the above reasons, certain (comatic) aberrations are not possible to represent faithfully in the model. In addition, the relationship between the sensor's MRC and target-acquisition performance does not hold when ghosts, flicker, or spatially coherent noise is present. However, spatially random, temporally coherent noise is modeled correctly.

REPORT DOCUMENTATION PAGE

Form Approved
OMB No. 0704-0188

1. REPORT DATE	2. REPORT TYPE	3. DATES COVERED *(From–To)*
November 2011	Final	June 2011 – November 2011

4. TITLE AND SUBTITLE

Conceptual Design of Low-Signature High-Endurance Hybrid-Electric UAV

5a. CONTRACT NUMBER
DASW01-04-C-0003

5b. GRANT NUMBER

5c. PROGRAM ELEMENT NUMBER

6. AUTHOR(S)

Jenya Macheret
Jeremy Teichman
Robert Kraid

5d. PROJECT NUMBER

5e. TASK NUMBER
CRP 2154

5f. WORK UNIT NUMBER

7. PERFORMING ORGANIZATION NAME(S) AND ADDRESS(ES)

Institute for Defense Analyses
4850 Mark Center Drive
Alexandria, VA 22311-1882

8. PERFORMING ORGANIZATION REPORT NUMBER

IDA Document NS D-4496
Log: H11-001789

9. SPONSORING/MONITORING AGENCY NAME(S) AND ADDRESS(ES)

Institute for Defense Analyses
4850 Mark Center Drive
Alexandria, VA 22311-1882

10. SPONSOR/MONITOR'S ACRONYM(S)

11. SPONSOR/MONITOR'S REPORT NUMBER(S)

12. DISTRIBUTION/AVAILABILITY STATEMENT

Approved for public release; distribution is unlimited. (9 October 2012)

13. SUPPLEMENTARY NOTES

14. ABSTRACT

The results of this investigation show the feasibility of designing a hybrid-electric unmanned aerial vehicle (UAV) that has low acoustic/visual signature and extended cruise flight endurance. The conceptual design is based on a small internal combustion engine that powers the cruise portion of the flight and an electric motor for loiter/intelligence, surveillance, and reconnaissance (ISR) portions. Relatively minor reductions in loiter mission duration produce a substantial increase in range. A decrease of 1 whr in the electric (loiter) energy onboard produces a gain of 13.3 whr in the gasoline (cruise) energy. These hybrid aircraft would allow extended range search-loiter-search missions, which are not possible with the existing electric UAVs.

15. SUBJECT TERMS

Hybrid-Electric UAV, flight endurance, wing aspect ratio, battery and IC engine weight, acoustic signature, thin electroluminescent film, IR payload.

16. SECURITY CLASSIFICATION OF:			17. LIMITATION OF ABSTRACT	18. NUMBER OF PAGES	19a. NAME OF RESPONSIBLE PERSON
					Mr. Philip Major
a. REPORT Uncl.	b. ABSTRACT Uncl.	c. THIS PAGE Uncl.	SAR	65	19b. TELEPHONE NUMBER *(include area code)* 703-845-2201